

Suxiao Jiuxin Pills, a Chinese herbal complex, block human potassium channel current hKv1.5 in CHO cells

Minzhou Zhang

University of Chinese Medicine, Guangdong Province Hospital of Chinese Medicine

Juan Yu

University of Chinese Medicine, Guangdong Province Hospital of Chinese Medicine

Jiashin Qu

Northeast Ohio Medical University

Jianyong Qi (✉ drqjy@163.com)

University of Chinese Medicine, Guangdong Province Hospital of Chinese Medicine

Research Article

Keywords: Kv1.5 channel, Ionic current, Gating current, Suxiao Jiuxin Pills

Posted Date: May 31st, 2022

DOI: <https://doi.org/10.21203/rs.3.rs-1671572/v1>

License:   This work is licensed under a Creative Commons Attribution 4.0 International License.

[Read Full License](#)

Abstract

Kv1.5 channel plays key roles in cardiac action potential and atrial repolarization. Suxiao Jiuxin Pills (SXJ), an herbal remedy had been widely used in China in treating angina pectoris and atrial arrhythmia. However, whether SXJ regulates Kv1.5 channels is still unclear. The goal of the present study was to examine the effects of SXJ on cloned human potassium channels (hKv1.5) in Chinese hamster ovary (CHO) cells. The ionic and gating currents were detected; dose-dependent curve, current-voltage curve, steady-state activation curve (SSA), activation time constant (τ_{act}), deactivation (τ_{deact}), and gating currents were compared between SXJ and control. Further, intracellular application of SXJ was implemented. Results showed that SXJ inhibited the hKv1.5 current in a time-, dose- and voltage-dependent manner with a half maximal inhibitive concentration (IC_{50}) value of 38.85 milligram per liter. The voltage dependence was described by an equivalent electrical distance δ of 0.15, which suggested that at the binding site SXJ experienced 15% of the applied transmembrane electrical field. There were no significant different changes of SSA, τ_{act} , τ_{deact} , 'On' gating current ($on-I_g$), and 'off' gating current ($off-I_g$) between SXJ and Control ($P > 0.05$). Intracellular application of SXJ could block the hKv1.5 current significantly ($P < 0.05$). In conclusion, SXJ produces a dose-, time-, and voltage-dependent block of hKv1.5, with interacting electrical distance δ of 0.15. SXJ did not influence the gating currents and deactivation time course. SXJ was an open-blocker, which provided the experimental research of SXJ in clinical treating atrial arrhythmia.

Introduction

The human Kv1.5 (hKv1.5) channel, a Shaker-type K⁺ channel, is encoded by the KCNA5 gene and expressed in a wide variety of tissues, including heart, brain, vascular, macrophages, etc (Lu et al. 2019; Doczi et al. 2016). hKv1.5, forms ultrarapid delayed rectifier K⁺ currents (I_{Kur}), is specifically expressed in human atrial but not in ventricular myocytes, plays an important role in the repolarization of atrial action potential (Ravens 2017). Reduction of hKv1.5 prolongs atrial action potential duration and may prevent atrial fibrillation (AF) and flutter. Moreover, it does not substantially prolong ventricular re-polarization or prolong the QT interval. Therefore, hKv1.5 blockers act as atrial-selective agent, can be a potential target and developing strategy for suppressing AF.

Each Kv1.5 alpha subunit consists of six transmembrane spanning segments (S1–S6) with intracellular amino and carboxy-termini. Voltage-dependent gating is associated with the movement of positive charges within the S4 segments (four arginine residues) in response to changes of the electrical field across the membrane. The 'voltage sensor' of the ion channel consists of parts of the S3 and S4 alpha helices that form a hairpin-like structure called the paddle motif (Catacuzzeno et al. 2020). The gating currents of hKv1.5 can provide additional information about the activation gating mechanism because they reflect transitions which are generally not observable with ionic currents. Various gating transitions will be helpful in the course of understanding drug binding which may interfere with these transitions, and

also in terms of understanding the implications of these transitions in the kinetics and voltage dependence of channel opening.

Suxiao Jiuxin Pill (SXJ), is made up of 2 herbal medicines, Rhizome *Ligusticum Chuan-xiong* (Chuanxiong, *Ligusticum chuanxiong Hort.*) and *Borneolum Syntheticum* (Bingpian)., has been widely used for treating angina pectoris, and atrial arrhythmia in China for more than 30 years (Duan et al. 2008). Researchers reported that SXJ could inhibit frequent atrial premature beats, junction premature beats, and AF (Yan et al. 2004). Others reported that SXJ could reduce reperfusion arrhythmia in mice (Tan et al. 2020). *Tetramethyl pyrazine*, an extract of *Chuanxiong*, can inhibit the L-type calcium currents in adult rat ventricular myocyte, and bind to the inactivated calcium channels (Ren et al. 2012). *Borneolum*, the other component of SXJ, can activate the volume sensitive chloride channels in nasopharyngeal carcinoma cells, and enhance human γ -aminobutyric acid currents expressed in *Xenopus* oocytes (Hall et al. 2004; Meng et al. 2014).

SXJ could reduce atrial arrhythmia with its effects on ion channels in cardiac myocytes (Bai et al. 2014). However, the effects of SXJ on hKv1.5 channel are still unclear. We hypothesized that responses of hKv1.5 could underlay the mechanisms of SXJ's effects on AF in the heart. Therefore, we examined the direct effects of SXJ on hKv1.5, expressed in Chinese hamster ovary (CHO) cells.

Materials And Methods

CHO cell culture and gene transfection

The CHO cells (American Type Culture Collection, USA) were grown in Dulbecco's modified eagle's medium/Ham's F-12 (DMEM, Invitrogen) supplemented with 10% fetal bovine serum (Gibco), 100 U/ml penicillin and 100 ug/ml streptomycin. The cell lines were maintained in a humidified incubator at 37°C with 5% CO₂. The human Kv1.5 cDNA in eGFP-contained GV230 vector was constructed by Shanghai Genechem Co., LTD. The hKv1.5 cDNA were transfected into CHO cells as previously reported (Schwetz et al., 2010). The cells were plated at 50–70% confluence on two 35 mm dishes 24 hours (h) prior to transfection with 1.6 ml Opti-MEM (Invitrogen) containing 8 μ l of lipofectamine (Invitrogen), and 2 μ g of plasmid DNA containing the human Kv1.5 (accession #: NM_002234) cDNA. Cells were incubated with the liposomal/DNA mixture at 37 °C in a 5% CO₂ humidified incubator. 6 to 12 hours post-transfection, the medium was replaced with F-12 medium. Cells were incubated at 37 °C for another 72 hours prior to commencing electrophysiological recordings, and 3-7 days could be maintained for patch-clamp experiments.

Whole-cell patch-clamp recording experiment

All experiments were carried out at room temperature (22–25°C). Membrane currents were recorded in voltage-clamp mode using an EPC-10 amplifier and Pulse software (HEKA, Lambrecht, Germany). Borosilicate glass electrodes (1.5mm OD) were pulled using a programmable horizontal microelectrode puller (PC-100; NARISHIGE Co., Japan). The patch pipette had a tip resistance of 3–5 M Ω when it was

filled with the pipette solution. The liquid junction potentials between extracellular and intracellular solutions were offset prior to formation of the seal. After a gigaohm seal was obtained, the cell membrane was ruptured by gentle suction to establish the whole-cell configuration. Whole-cell capacitive current compensation and 60-80% series resistance compensation were optimized with leak subtraction. Current signal was sampled at 10 kHz, recorded and stored in the hard disk of a PC compatible computer.

Steady-state activation curves (SSA) were derived by normalizing the tail currents at -40 mV after stepping the depolarizing voltage from -60 to +50 mV. The activation curves were fitted with the Boltzmann equation: $Fraction\ of\ maximal\ current = [1 + \exp[-(V-V_a)/K_a]]^{-1}$, where V_a is the potential when the conductance is half-activation, V is the test potential, and k_a represents the slope factor for the activation curve. The concentration response relationship for the current activation by SXJ was fitted to the Hill equation: $f = 1/[1+(D)/(IC_{50})^{n_H}]$, where f is the fractional inhibition at various SXJ concentrations, half-maximal inhibitive concentration (IC_{50}) is the SXJ concentration at median activation concentration, D is the SXJ concentration, and n_H is the Hill coefficient.

Solutions of gating currents and pulse protocols

For gating current experiments (Fedida **1997**), cells were superfused with a solution containing (mM): 140 N-methyl-D-glucamine(NMDG), 10 Hepes, 1 CaCl₂, 1 MgCl₂, 10 dextrose, adjusted to pH 7.4 with HCl. The pipette solution contained (mM): 140 NMDG, 10 Hepes, 1 MgCl₂, 10 EGTA, adjusted to pH 7.2 using HCl.

For whole-cell recording of hKv1.5 ionic currents (Jeong et al. **2010**), the bath solution contained (in mM) 140 NaCl, 5 KCl, 1 MgCl₂, 1 CaCl₂, and 10 HEPES, adjusted to pH 7.3 with NaOH. The pipette solution contained (in mM) 140 KCl, 1 CaCl₂, 1 MgCl₂, 10 HEPES, and 10 EGTA, adjusted to pH 7.3 with KOH. SXJ was provided by the Sixth Chinese Drugs Factory of Tianjin Zhongxin Pharmaceutical Co., Ltd.(Tianjing, China, batch No. 6015158). SXJ was vortexed, dissolved in sterile distilled water, and filtered as a stock solution of 30 mg/mL, and then the concentration used in the current study was diluted with the extracellular solution to obtain the desired concentrations.

To examine the voltage dependence of Kv1.5 inhibition by the drug, the fractional inhibition was measured at individual test potentials and the voltage dependence of the fractional inhibition was fitted with a Woodhull equation (Woodhull **1973**): $f = [D] / \{ [D] + K_d(0) \cdot \exp(-z\delta FV/RT) \}$ where $K_d(0)$ is the apparent affinity at 0 mV (the reference voltage), z is the charge valence of the drug, δ is the fractional electrical distance (i.e., the fraction of the transmembrane electric field sensed by a single charge at the receptor site), F is Faraday's constant, R is the gas constant, and T is the absolute temperature. In the present study, 25.4 mV was used as the value of RT/F at 22°C. Activation time constants were determined by fitting the current traces that were used to measure the I-V relationships. Whole cell current traces were fitted to a fourth power exponential function to determine τ_n . Cells were superfused continually at a flow rate of 1–2 ml/min (Chen and Fedida. **1998**). After control data were obtained, bath perfusion was switched to drug-containing solution. Drug infusion or removal was monitored with test pulses from -80 mV to +50 mV, applied every 30 s until steady state was obtained (within 5-15 min, Snyders et al., **1992**).

Data analysis and statistics

Data analysis was done using PatchMaster (HEKA) and Origin 8.0 software (Origin Lab Corp., Northampton, MA, USA). All values were expressed as means \pm SEM. One-way analysis of variance, followed by the Bonferroni test for comparisons of multiple groups, was used for statistical analysis. P values were considered significant at $p < 0.05$.

Results

Concentration-dependent block

To explore the effect of SXJ on the hKv1.5 current, we implemented the whole cell patch clamp experiments in CHO cells. Fig. 1e showed the protocol that depolarization were ranged from -50 mV to $+50$ mV in 10 mV increments with 250 -ms duration from a holding potential of -80 mV. As shown in Fig.1a, under control conditions, the hKv1.5 currents rose instantaneously and declined slowly, which meant that the hKv1.5 currents owned a fast activation followed by a slow inactivation. Fig.1b showed the effects of application of 30 mg/L SXJ, which reduced the hKv1.5 current slightly, without significantly decay changes. When superfusion of 300 mg/L SXJ, hKv1.5 current significantly reduced with significantly decay, which meant a fast inactivation after 300 mg/L SXJ stimulation (Fig.1c). Fig.1f showed the different concentrations of SXJ (10 – 300 mg/L) blocked the peak currents of steady-state hKv1.5 currents. According to the Hill equation (equation in Materials and Methods), the data points of the peak currents yielded an IC_{50} value of 38.85 ± 1.06 mg/L with n_H of 1.2 ± 0.1 ($n=5$). A Hill coefficient value that approaches 100% indicate that one molecule of SXJ is sufficient for activation of a single hKv1.5 channel. To examine the reversibility of the effect of SXJ, the time course for alteration in steady-state currents produced by the drug of SXJ and by ensuing drug washout was analyzed (Fig. 1d). When a drug-free solution was changed to a drug-containing solution, steady-state inhibition of Kv1.5 was abolished. This indicates that the effect of SXJ on hKv1.5 is time-dependent and reversible.

Voltage-dependent block and time course of tail current

To ensure the voltage-dependent relationships of SXJ effects on hKv1.5 in CHO cells, patch clamps experiments were implemented with activation protocols. Fig. 2a showed the effect of 100 mg/L SXJ on the steady state current-voltage (I-V) relationship. Under the control conditions, the hKv1.5 channel was activated from -30 mV and its amplitude increased linearly with depolarization. In the presence of SXJ, the amplitude of the hKv1.5 current was blocked from -30 mV, and significantly inhibited with the depolarized increments. This is indicative of more extensive block at the larger depolarization.

To quantitate this voltage dependence, the relative current $I_{SXJ}/I_{control}$ and the effect of the transmembrane electrical field (δ) on the interaction were plotted as functions of voltage (Fig. 2b). The inhibition of the Kv1.5 current ($I_{SXJ}/I_{control}$) was increased with the voltage augmented. The δ was calculated by using a simple Woodhull equation (see Materials and methods). The solid line in Fig. 2b denotes a fit curve, which yielded a δ value of 0.15 ± 0.05 ($n=8$).

To further examine the voltage-dependent inhibition of Kv1.5, the effect of SXJ on deactivation kinetics was analyzed. In Fig. 2c above, the protocol showed the control tail current traces obtained by a 250-ms repolarizing return pulse of -40 mV after a 250-ms depolarizing pulse of $+50$ mV from a holding potential of -80 mV, the tail trace was fitted to a single exponential function. Under control conditions, the tail current declined, with a time constant of 55.06 ± 2.30 ms (Fig.2d, $n= 16$). In the presence of 100 mg/L SXJ, the initial amplitude of the tail current was decreased and the subsequent decline of the tail current was considerably slowed with a deactivation time constant of 56.49 ± 3.06 ms ($n= 9$, $p > 0.05$).

Steady-state activation and activation time constant

To ensure whether SXJ effects on the activation state of hKv1.5 in CHO cells, the voltage dependence of steady-state activation of hKv1.5 was evaluated by tail current analysis with a two pulse protocol in the absence and presence of SXJ (Fig. 3a-b). The picture above Fig. 3a showed the protocol of a series of depolarizing potentials were administered from -60 to $+50$ mV with 100 ms steps, followed by a potential at -40 mV for 250 ms, and finally returned to the holding potential of -80 mV. The normalized tail currents were fitted to the Boltzmann equations. The potentials for the half activation point (V_a) and slope factor (K_a) of the steady state activation curve were -16.35 ± 0.87 and 12.51 ± 0.82 mV for the control ($n = 12$), and -18.90 ± 1.10 and 13.14 ± 1.02 mV for the 100 mg/L SXJ ($n=8$), respectively (Fig. 3c). The data indicated that there was no depolarizing shift in the voltage at which hKv1.5 activated. Moreover, the activation time constant (τ_{act}) was compared. the τ_{act} In response to 100 mg/L SXJ was not significantly altered compared with the control group (Fig.3d), which indicated that there were no significantly changed from close to open state.

Effects of SXJ on hKv1.5 gating currents

To observe the rapid block ($5-15$ ms) of SXJ that cannot be detected from ionic current data, the gating current experiment was implemented. Fig. 4a-c illustrated the actions of $30-300$ mg/L SXJ on gating currents. The cells were pulsed from -100 to $+50$ mV for 12 ms to record the on-Ig, and then back to -100 mV to record the off-Ig (picture above Fig. 4a). As shown in Fig. 4a, the control gating currents were marked with the black line while the SXJ gating currents were marked with the red line. The SXJ group was nearly overlapped with the control group, which suggested that there was little effect of SXJ on on-Ig at any concentration, also similar dose-dependent action on off-Ig. The integrals of the currents on-Ig (Q_{on}) and off-Ig (Q_{off}) at $30-300$ mg/L SXJ in Fig. 4a-c were shown in Fig. 4d. Q_{on} , and Q_{off} were quite symmetrical and equal in magnitude in control and SXJ groups. Moreover, with the test potential increased from -70 mV to $+50$ mV, the ratio of Q_{off}/Q_{on} was still not change among the control and these three SXJ dosages ($30,100,300$ mg/L). These results indicated that Q_{off}/Q_{on} was unchanged in the presence of SXJ, no matter dose-dependent or voltage-dependent. These values were generally in agreement with the ionic data (Fig. 3c) and provide support for the conclusion that SXJ did not influence the voltage sensor and the close to open states.

Intracellular application of SXJ on hKv1.5

Since both active ingredients (Rhizome *Ligusticum Chuan-xiong* and *Borneolum Syntheticum*) of SXJ are lipophilic, it is possible that the ingredients permeates the plasma membrane and binds to intracellular hKv1.5 channel protein. It is not clear whether this effect were mediated via a cell surface binding site, or an intracellular site. To test the possibility, CHO cells were perfused intracellularly with the patch pipette solution containing different concentrations of SXJ (30, 100, 300 mg/L, respectively). The amplitudes of the hKv1.5 currents were plotted (Fig. 5a). The cells were pulsed from -80 to +50 mV for 250 ms to record the hKv1.5 channel current (picture above Fig. 5e). As shown in Fig.5a-d, with the concentrations of SXJ increased, the peak amplitude was decreased followed by augmented decay. The hKv1.5 current was significantly inhibited after 30 mg/L SXJ superfusion, which was more effective compared with extracellular stimulation (Fig. 1). Therefore, intracellular SXJ exerted significantly inhibitory effects on the hKv1.5 channel currents, suggesting that the SXJ binding site is located on the intracellular surface.

Discussion

The present study illustrated the effect of SXJ on hKv1.5 in CHO cell. Our results can be summarized as followed: (1) SXJ could block hKv1.5 current in voltage-, time-, and dose-dependent manners, with the IC_{50} is 38.85 mg/L; (2) SXJ could fasten the inactivation with electrical distance $\delta = 0.15$, suggested that at the binding site SXJ occupied 15% of the applied transmembrane electrical field; (3) SXJ had no significant effects on steady-state activation, τ_{act} and τ_{deact} ; (4) SXJ had no significant effects on hKv1.5 gating currents (on-Ig and off-Ig); (5) SXJ interacted at the internal mouth of the pore of the hKv1.5 channel and blocked the hKv1.5 currents.

Our study suggested that SXJ could bind to the open state of the hKv1.5 channel, which was due to three reasons. Firstly, the initial time course of activation and the τ_{act} were not modified compared with the control group (Fig. 1 and Fig. 3d); Secondly, block mainly occurred after the hKv1.5 channel opening, since the amplitude of the hKv1.5 current was blocked from the beginning of -30 mV, which was just the initial stage of the hKv1.5 channel opening (Fig. 2a); Finally, the block of the hKv1.5 channel current by SXJ was increased sharply in the voltages ranged of the hKv1.5 channel activation, which was varied from - 30 mV to + 50mV (Fig. 2b).Therefore, these data suggested that SXJ could bind and block the open state of the hKv1.5 channel.

In the present study, it was found that SXJ could fasten the inactivation state of the hKv1.5 channel current. In the control group, during depolarization, it was induced fast activation followed by slowly single exponential decay (Fig. 1a, C-type inactivation). However, In the presence of SXJ (Fig. 1c), the inactivation state became biexponential, the inactivation state was fastened after SXJ superfusion with significantly big decay. The SXJ-induced extra componenet of inactivation had a time constant that was faster than that of slow inactivation of the control group. Thus, we suggested this fast time constant might be due to the interaction of SXJ with the open state of the hKv1.5 channel.

Although SXJ affects the inactivation time course of the hKv1.5 current during depolarization, it did not modify the tail current significantly. Due to slightly occupied the binding site of the open state, SXJ just

moved 15% into the membrane electrical field to the receptor and blocked the hKv1.5 channel current (Fig. 2b, $\delta = 0.15$). In general, the δ varied among 0.19 ~ 0.32, can be interpreted to indicate that drugs moves about 19 ~ 32% into the membrane electrical field to reach the receptor and block ion current, such as quinine, tetrapentylammonium, methoxamine, etc (Snyders and Yeola. **1995**; Parker et al. 1999). Therefore, SXJ did not result in a initially rising phase of the tail current, followed by a slowly decline. Because SXJ just occupied a little fraction of the open channel, it went more to closing state when depolarization. In the control group, upon repolarization at -40 mV, the hKv1.5 potassium current deactivated completely, with a time constant of 55.06 msec. This time constant reflects mainly the virtually irreversible closing of the channel. In the response of SXJ, the tail declined with a time constant of 56.49 ms, which had not significantly different changes compared with the control group ($p > 0.05$, Fig. 2d), thus did not resulting in a “crossover” phenomenon (Brown et al. **1980**). Our study was similar with Li’s publication (Li and Aldrich 2004). Li intracellularly applied quaternary ammonium (QA) compounds to probe the pore of Large conductance Ca^{2+} -activated K (BK) channels, and found that large QA molecules “trapped” inside during repolarization, blocked BK channels without slowing the overall process of deactivation. Therefore, SXJ blocked the open channel of the hKv1.5 current, without affected the deactivation process.

The ionic current data indicated that SXJ did not alter the channel activation (Fig. 3c-d), but high concentrations of SXJ started to block hKv1.5 channels (Fig. 1b-c) meant that it was difficult to exclude a SXJ action on intermediate closed states. One way to examine SXJ action on closed channels and kinetic states leading to the open state is to study the hKv1.5 channel gating current. Channel gating in voltage-dependent ion channels is transduced by the movement of regularly spaced, charged amino acids within the membrane capable of sensing the local potential drop across the lipid bilayer (Sigworth, 1994). The movement of these charges generates small currents that give information about the conformational changes in hKv1.5 channel subunits that occur as the channel moves towards the open state (Bezanilla et al. 1991). Currents rise very rapidly to reach larger peaks for greater depolarizations. Decay of currents was observed within 5–10 ms. In the present study, the effects of increasing doses of SXJ on gating currents and charge moved (Q_{on} and Q_{off}) are shown in Fig. 4a-d. The peak on-Ig, Q_{on} , off-Ig and Q_{off} were unaffected at various potentials and different concentrations of SXJ (Fig. 4d-e), these data provided evidence for a SXJ binding site on hKv1.5 channels that is exposed only when the channel opens. Therefore, the gating current experiments supported the idea that SXJ does not block the close channel, bound to the external vestibule of the channel so as to interfering with closure of the activation gate, and did not result in the “foot-in-the-door” phenomenon (Yeh and Armstrong. **1978**). Moreover, our study found that SXJ block the hKv1.5 channel from the intracellular site (Fig. 5), supporting SXJ function as an open channel blocker with binding sites in the inner cavity of the pore and access from the intracellular side.

Kv1.5 channels are the molecular correlate of $I_{K_{ur}}$ in human cardiomyocytes. Since $I_{K_{ur}}$ is prominent in atria and negligible in ventricle, it has been proposed as a safe ‘atria-selective’ drug target in supraventricular tachyarrhythmias (Burashnikov and Antzelevitch. **2009**). Indeed, many drug companies have developed selective $I_{K_{ur}}$ blockers for safe conversion of AF into sinus rhythm without much effect on

ventricular AP duration that could cause torsades de pointes arrhythmias. The biphenyl derivative AVE0118 blocks I_{Kur} in atrial myocytes and effectively prevents inducibility of AF episodes (Blaauw et al. 2004) and also converts chronic AF to sinus rhythm (de Haan et al. 2006). The two compounds S9947 and S20951 possess good selectivity of I_{Kur} block, and almost completely suppress left atrial vulnerability against AF induced by pre-mature stimuli in an in vivo model of anaesthetized pigs (Knobloch et al. 2002). The results of the present study suggest that SXJ blocks hKv1.5 in a concentration-dependent manner, providing a rationale for the potential therapeutic use of SXJ in the treatment of AF.

Since SXJ is a complex compound of natural herbs, it is hard to differentiate the precisely effects of components of SXJ in the present study. Moreover, it is also unclear whether SXJ could affect other ionic channels, such as BKCa, voltage-dependent sodium channel, L-type calcium channel, rapid and slow delayed rectifier potassium channels. Future studies will focus on whether SXJ plays a role on BKCa and other channels.

Conclusion

In summary, the present study, for the first time, showed that SXJ preferentially bound to and blocked hKv1.5 channels and caused a voltage-, time-, and dose-dependent inhibition of hKv1.5. These result experimentally revealed the effectiveness of SXJ as a clinical therapy to treat AF.

Abbreviations

SXJ, Suxiao Jiuxin Pills; CHO, Chinese hamster ovary; IC_{50} , Half maximal inhibitive concentration; hKv1.5, human Kv1.5 potassium channel; AMI, Acute myocardial infarction; DMEM, Dulbecco's modified eagle's medium; τ_n , Activation time constants; I-V, current-voltage; AF, atrial fibrillation.

Declarations

Author contributions

JW drafted this manuscript. JQ and JY performed the experiments. JW revised the manuscript, MZ contributed to the rationalization of the study. All authors read and approved the final manuscript

Acknowledgement

This work was supported by the National Natural Science Foundation of Guangdong (#2020A1515010777 to J.Y.).

References

1. Bai, X.Y., Zhang, P., Yang, Q., Liu, X.C., Wang, J., Tong, Y.L., Xiong, S.J., Liu, L.H., Wang, L., He, G.W., 2014. Suxiao Jiuxin Pill induces potent relaxation and inhibition on contraction in human artery and the mechanism. *Evid Based Complement Altern Med.* 2014, 956924.
2. Bezanilla, F., Perozo, E., Papazian, D.M., Stefani, E., 1991. Molecular basis of gating charge immobilization in Shaker potassium channels. *Science* 254, 679–683.
3. Blaauw, Y., Gogelein, H., Tieleman, R.G., van Hunnik, A., Schotten, U., Allessie, M.A. 2004. 'Early' class III drugs for the treatment of atrial fibrillation: efficacy and atrial selectivity of AVE0118 in remodeled atria of the goat. *Circulation* 2004;110:1717–1724.
4. Brown, H., DiFrancesco, D., Noble, D., Noble, S. 1980. The contribution of potassium accumulation to outward currents in frog atrium. *J Physiol.* 306, 127 – 49.
5. Burashnikov, A., Antzelevitch, C. 2009. Atrial-selective sodium channel block for the treatment of atrial fibrillation. *Expert Opin Emerg Drugs.* 14, 233–249.
6. Catacuzzeno, L., Sforna, L., Franciolini, F. 2020. Voltage-dependent gating in K channels: experimental results and quantitative models. *Pflugers Arch.* 472, 27–47
7. Chen, F. S., Fedida, D. 1998. On the mechanism by which 4-Aminopyridine occludes quinidine block of the cardiac K⁺ channel, hKv1.5. *J Gen Physiol.* 111, 539 – 54.
8. de Haan, S., Greiser, M., Harks, E., Blaauw, Y., van Hunnik, A., Verheule, S., Allessie, M., Schotten, U. 2006; AVE0118, blocker of the transient outward current (I_{to}) and ultrarapid delayed rectifier current (I_{Kur}), fully restores atrial contractility after cardioversion of atrial fibrillation in the goat. *Circulation.* 114, 1234–1242.
9. Doczi, M.A., Vitzthum, C.M., Forehand, C.J., 2016. Developmental expression of Kv1 voltage-gated potassium channels in the avian hypothalamus. *Neurosci Lett.* 616, 182–8.
10. Duan, X., Zhou, L., Wu, T., Liu, G., Qiao, J., Wei, J., Ni, J., Zheng, J., Chen, X.Y., Wang, Q., 2008. Chinese herbal medicine Suxiao Jiuxin Wan for angina pectoris. *Cochrane Database Syst Rev.* 23, CD004473.
11. Fedida, D. 1997. Gating charge and ionic currents associated with quinidine block of human Kv1.5 delayed rectifier channels. *J Physiol.* 499, 661–75.
12. Hall, A.C., Turcotte, C.M., Betts, B.A., Yeung, W.Y., Agyeman, A.S., Burk, L.A., 2004. Modulation of human GABAA and glycine receptor currents by menthol and related monoterpenoids. *Eur J Pharmacol.* 506, 9–16.
13. Jeong, I., Choi, B.H., Hahn, S.J. 2010. Effects of lobeline, a nicotinic receptor ligand, on the cloned Kv1.5. *Pflugers Arch.* 460, 851–62.
14. Knobloch, K., Brendel, J., Peukert, S., Rosenstein, B., Busch, A.E., Wirth, K. J. 2002. Electrophysiological and antiarrhythmic effects of the novel I_{Kur} channel blockers, S9947 and S20951, on left vs. right pig atrium in vivo in comparison with the IKr blockers dofetilide, azimilide, d,l-sotalol and ibutilide. *Naunyn Schmiedebergs Arch Pharmacol.* 366, 482–487.
15. Li, W., Aldrich, R. W. 2004. Unique inner pore properties of BK channels revealed by quaternary ammonium block. *J Gen Physiol.* 124, 43–57.

16. Lu,G., Li,J., Zhai,Y., Li,Q., Xie,D., Zhang,J., Xiao,Y., Gao,X., 2019.Spironolactone suppresses aldosterone-induced Kv1.5 expression by attenuating mineralocorticoid receptor-Nox1/2/4-mediated ROS generation in neonatal rat atrial myocytes. *Biochem Biophys Res Commun.*520,379–384.
17. Meng, L., Wang, H.B., Deng, Z.Q., Wang, Y., Wu, J.B., Lai, Z.Y., Lv, R.L.,Sun, X.X., Zhu, L.Y., Chen, L.X., Wang, L.W.,2014. Activation of Borneol on volume sensitive chloride channels in nasopharyngeal carcinoma cells. *Chinese Pharmacological Bulletin.*30,1671-6.[Chinese]
18. Parker, C., Li, Q., Fedida, D. 1999. Non-specific action of methoxamine on Ito, and the cloned channels hKv 1.5 and Kv 4.2. *Br J Pharmacol.* 126, 595–606.
19. Ravens U. Atrial-selective K + channel blockers: potential antiarrhythmic drugs in atrial fibrillation? *Can J Physiol Pharmacol.* 2017 Nov;95(11):1313–1318.
20. Ren, Z., Ma, J., Zhang, P., Luo, A., Zhang, S., Kong, L., Qian, C.,2012. The effect of ligustrazine on L-type calcium current, calcium transient and contractility in rabbit ventricular myocytes. *J Ethnopharmacol.*144,555 – 61.
21. Schwetz, T.A., Noring, S.A., Bennett, E. S. 2010. N-glycans modulate K(v)1.5 gating but have no effect on K(v)1.4 gating. *Biochim Biophys Acta.* 1798, 367–75.
22. Sigworth, F.J., 1994. Voltage gating of ion channels. *Q. Rev. Biophys.* 27, 1–40.
23. Snyders, J., Knoth, K. M., Roberds, S. L., Tamkun, M. M. 1992. Time-, voltage-, and state-dependent block by quinidine of a cloned human cardiac potassium channel. *Mol Pharmacol.* 41, 322–30.
24. Snyders, D. J., Yeola, S. W. 1995. Determinants of antiarrhythmic drug action. Electrostatic and hydrophobic components of block of the human cardiac hKv1.5 channel. *Circ Res.* 77, 575–83.
25. Tan, Y.F., Yu, J., Pan, W.J., Qi, J.Y., Zhang, M.Z.,2020.Protective Mechanisms of Suxiao Jiuxin Pills on Myocardial Ischemia-Reperfusion Injury in vivo and in vitro.*Chin J Integr Med.* 26,583–590.
26. Woodhull, A. M. 1973. Ionic Blockage of Sodium Channels in Nerve. *J Gen Physiol.*61,687–709.
27. Yan, J., He Z. 2004. Clinical observation of Suxiao Jiuxin Pills on arrhythmia. *Practical Clinical Medicine.* 5, 43–44.[Chinese]
28. Yeh, J. Z., Armstrong, C.M. 1978. Immobilisation of gating charge by a substance that simulates inactivation. *Nature.* 273, 387–389.

Figures

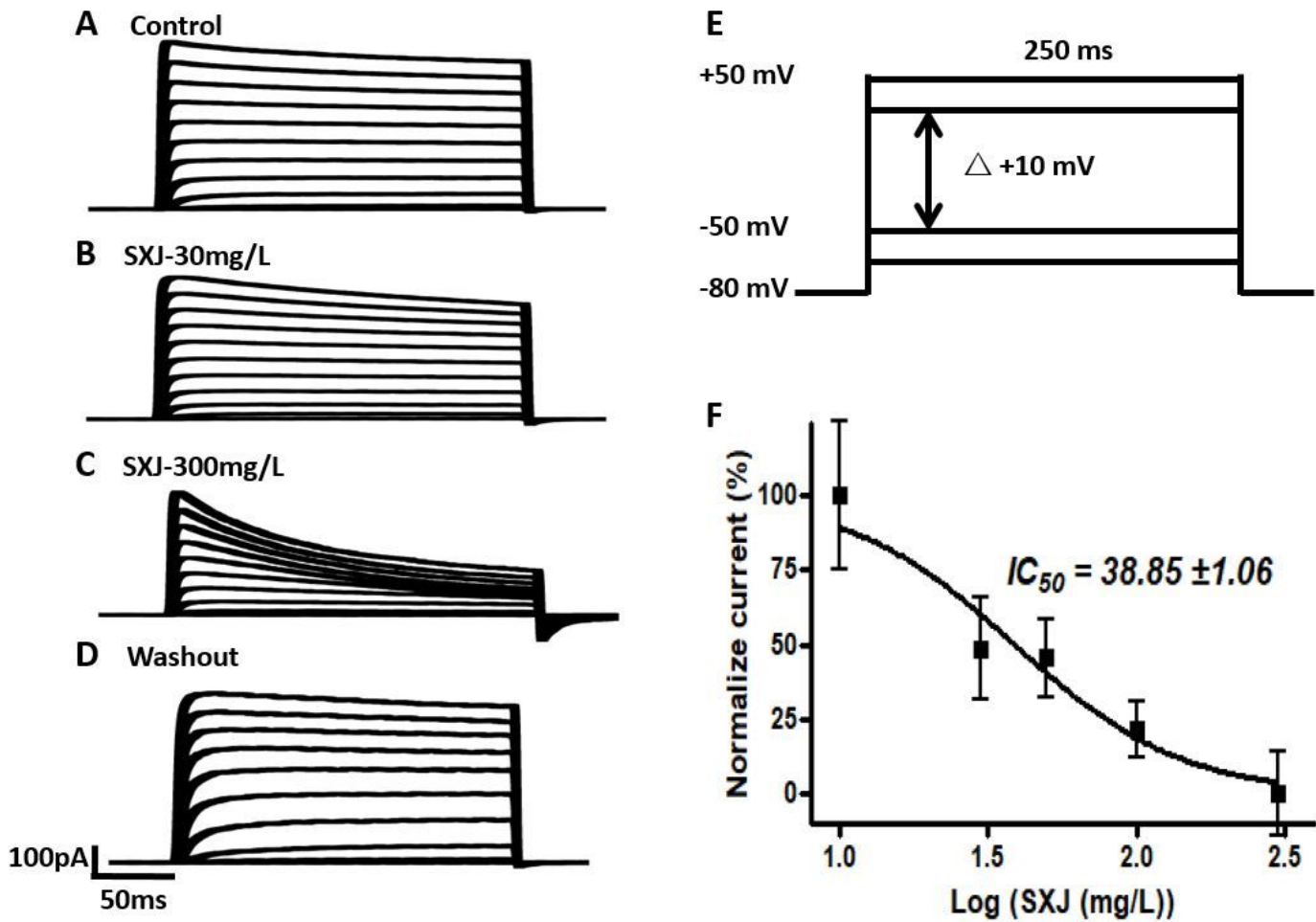


Figure 1

Reduction of hKv1.5 current by SXJ. Currents are shown from (a) control, (b) 30mg/L SXJ, (c) 300mg/L SXJ,(d) washout, respectively.(e) voltage protocol was from -50 to +50 mV in 250ms, 10mV increments.. (f) Normalized currents were fitted to the Hill equation and $IC_{50} = 38.85$ mg/L.

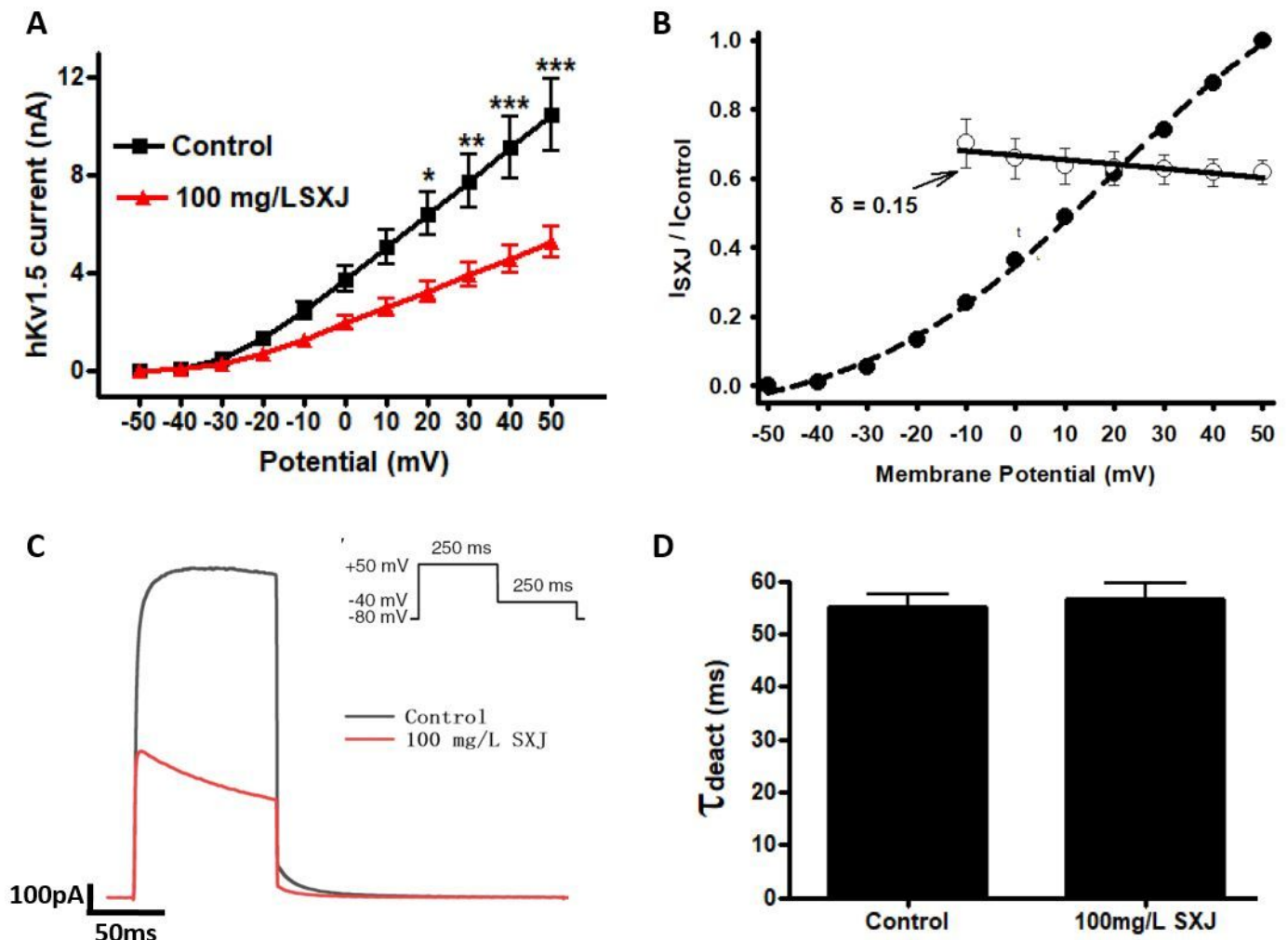


Figure 2

Current–voltage curve and deactivation of hKv1.5 by SXJ. (a) I–V curve of hKv1.5 between control and 100 mg/L SXJ; (b) Relative current ($I_{SXJ}/I_{Control}$) calculated from data in a. (c) Tail currents were recorded during a -40 mV, 250-ms repolarizing pulse after a +50mV, 250-ms depolarizing pulse in control and SXJ. (d)

The deactivation time constants (τ_{deact}) were compared between control and SXJ ($p > 0.05$). Data are expressed as the means \pm SEM.

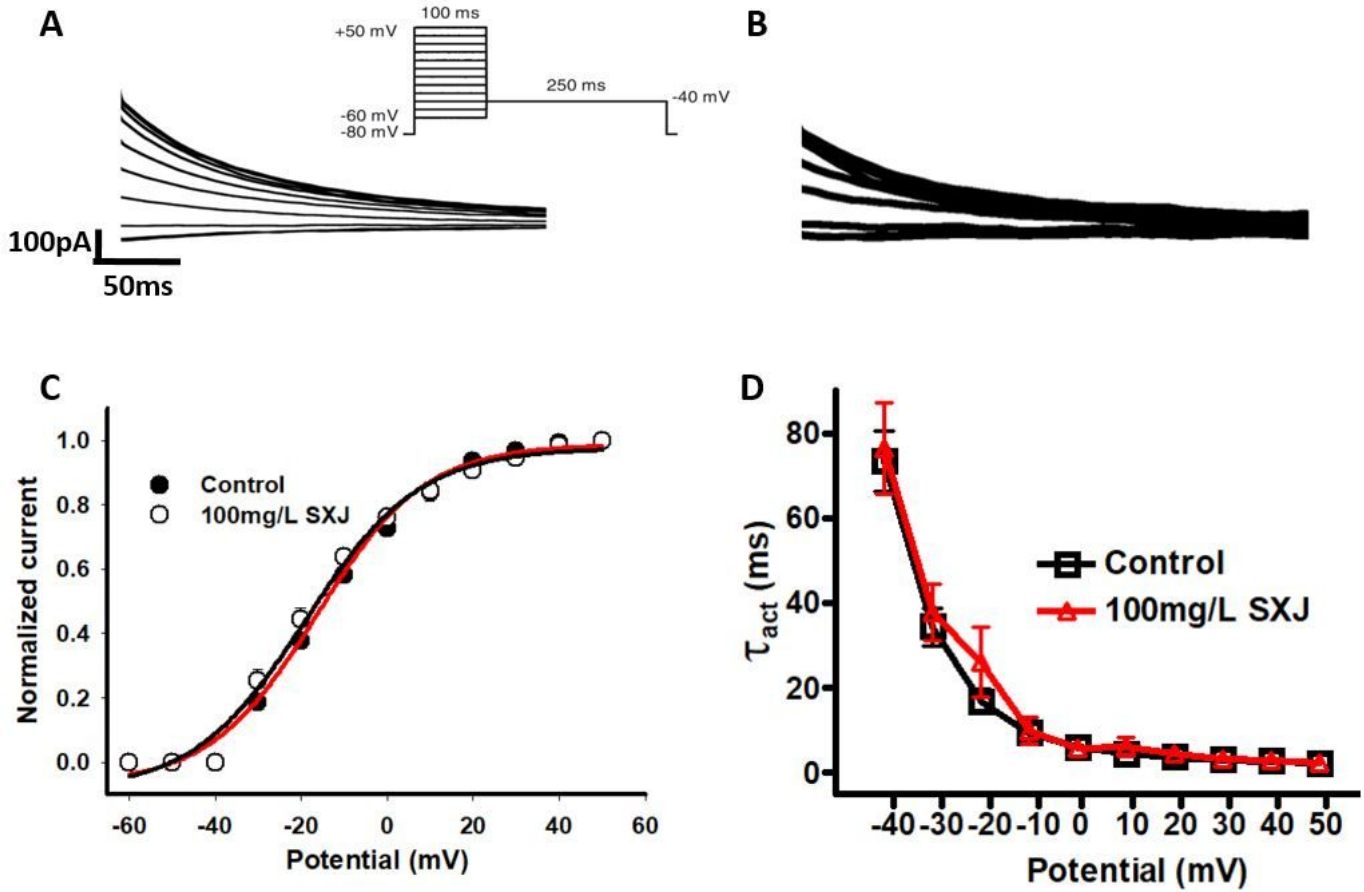


Figure 3

Steady-state activation curve of hKv1.5 by SXJ. Superimposed currents were elicited in control (a) and SXJ (b). Voltage protocol was listed at -40 mV for 250ms after 100-ms stepping depolarizing pulses from -60 to +50 mV. (c) Tail currents were normalized to their maximal values before each set of data was fitted to the Boltzmann equation. (d) Activation time constants (τ_{act}) were compared between control and SXJ ($p > 0.05$). Data are expressed as the means \pm SEM.

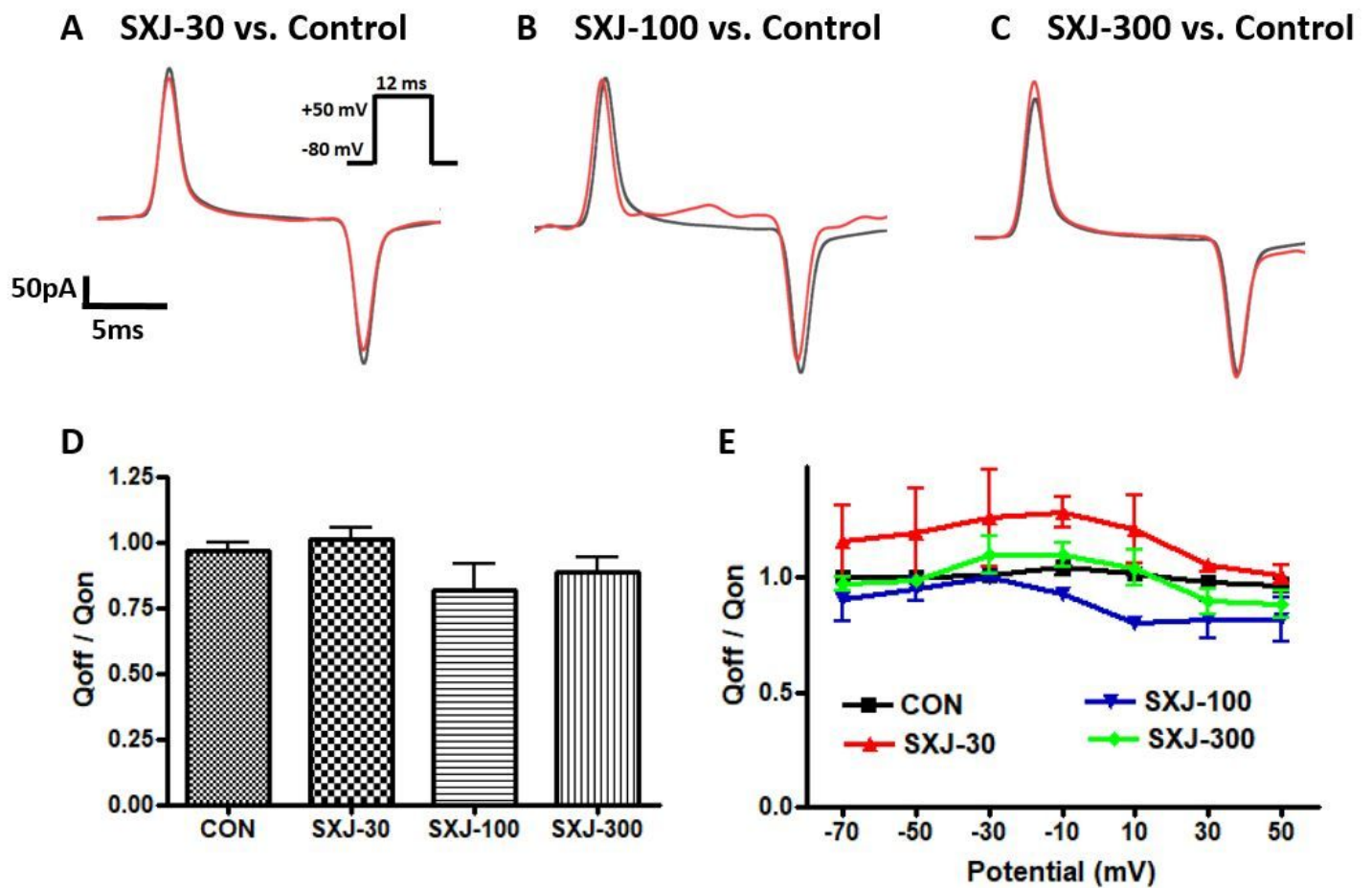


Figure 4

Gating currents of hKv1.5 were not altered by SXJ. Superimposed gating currents were elicited in 30mg/L (a), 100mg/L (b), and 300 mg/L SXJ (c, red line) overlapped with control (black line). Voltage protocol was listed at +50 mV for 12ms. (d) The ratio of off-gating charge (Q_{off}) on-gating charge (Q_{on}) were compared among the 4 groups (con, 30, 100, 300 mg/L SXJ, respectively, $p > 0.05$). (e) The ratios of Q_{off}/Q_{on} of the 4 groups were unchanged with the voltages increased. ($p > 0.05$). Data are expressed as the means \pm SEM.

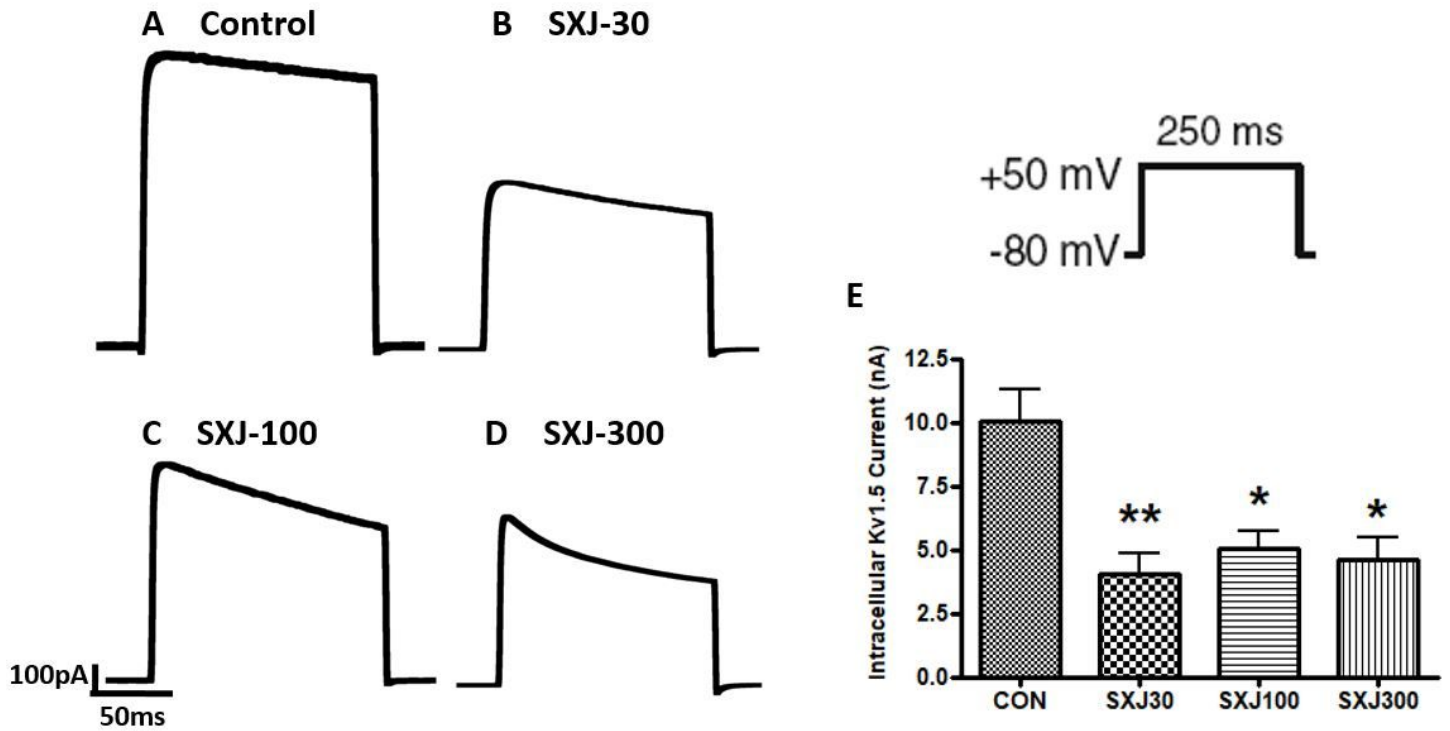


Figure 5

Intracellular application of SXJ reduced the hKv1.5 currents. Voltage protocol was listed at +50 mV for 250ms with the -80 mV holding potential. Superimposed currents were elicited in control (a), 30mg/L (b), 100mg/L (c), and 300 mg/L SXJ (d) respectively. (e) The peak amplitude of the hKv1.5 currents were compared among the 4 groups. * $p < 0.05$, ** $p < 0.01$, compared with control. Data are expressed as the means \pm SEM.